TECHNIUM

Technium Vol. 2, Issue 4 pp.33-38 (2020)
ISSN: 2668-778X
www.techniumscience.com

Evaluation of modulus of elasticity, nano-hardness and stiffness of TiCN coating deposited by PACVD

S.M.M.SHAFIEI[1, 2], M.DIVANDARI[1], S.M.A.BOUTORABI[1, 3]
[1]School of Metallurgical Engineering, Iran University of Science and Technology, Tehran, Iran
[2]Islamic Azad University, Rudehen Branch, Tehran, Iran
[3]Center of Excellence for High Strength Alloys Technology, Tehran, Iran
Dr.smm.shafiei@gmail.com

Abstract. Modulus of elasticity (E) and nano-hardness (H) of the TiCN coating deposited on AISI H12 steel by plasma assisted chemical vapor deposition (PACVD) have been measured from load–displacement curves, resulting from nano-indentation testing. Stiffness (S) of the coatings has been evaluated from the indentation method. A qualitative evaluation of interfacial strength between coating and substrate material was also performed by indentation method. Results indicated elastic modulus and stiffness of the coatings are in the range of 97.3–99.2 GPa and 67.8–70.6 MPam1/2 those are respectively lower and higher than those of the individual constituent ceramics.
Keywords: *Nano-indentation, Modulus of elasticity, Stiffness, Ratio of hardness and elastic modulus (H/E)*

1. Introduction

TiCN has received considerable attention as coating materials in the past for their inherent advantages like high hardness and wear resistance [1–9]. However, due to low fracture toughness and high modulus of elasticity, these coatings, when used individually, may not prove to be wise choices for coating applications [10]. This beneficial property of ternary coating can be utilized to develop coatings with high wear resistance coupled with high strength. Plasma-assisted coating is a surface modification process characterized by high processing speed, controlled precision, and by its applicability in case of most of the coating materials. High depositing rates attainable in plasma processing give rise to extremely refined microstructures leading to improved mechanical properties [6].

Extensive work has been done so far by various research groups, to develop novel coatings with high hardness and high wear resistance by plasma surface engineering [11–17]. However, the major portion of the research attention in this field is focused towards the characterization of microstructures, determination of micro-hardness and the evaluation of triboligical behavior. The modulus of elasticity (E) and stiffness (S) of a coating material are important properties that determine the mechanical strength of the coating. In addition, induced residual stress of the composite coating is dependent on the elastic modulus. For a coating, E changes according to composition of the material as well as the processing technique adopted. As measurement of modulus of elasticity (E) is cumbersome and almost impossible by utilizing conventional methods for such limited-area, low-thickness coating, and nanoindentation technique is widely employed. Analysis of the indentation load–displacement curves resulting from the nanoindentation test are effectively used in the evaluation of various mechanical properties like hardness, modulus of elasticity, scratch resistance, residual stress, etc. [18]. Oliver and Pharr [19] developed a mathematical model to evaluate nano-hardness and modulus of elasticity by analysis of the indentation load–displacement curves resulting from the nanoindentation test. Most of

the previous studies concerning determination of hardness and modulus of elasticity by nanoindentation techniques were evaluated either on thin films [20–23] or on bulk ceramics or ceramic composite materials [24–26]. Very few of the reported investigations [27–29] on the evaluation of these properties were carried out on coatings developed by plasma technology. Biswas et al. [27] calculated the hardness and Young's modulus from aload–displacement graph using the method proposed by Oliver and Pharr for TiN coating on Ti–6Al–4V alloy developed through plasma nitriding. Agarwal and Dahotre [28] determined modulus of elasticity and hardness using nanoindentation technique for composite boride coatings developed by plasma surface alloying. Elastic modulus values of the coating were correlated with the reaction(s) occurring within the coating region due to different plasma processing conditions.

In the present work, the modulus of elasticity (E) and nano-hardness (H) of the TiCN coatings have been evaluated from load–displacement curves resulting from nanoindentation test assessed in conjunction with the method developed by Oliver and Pharr [19]. Stiffness of the coating has been calculated from the method developed by Evans and Wilshaw [32]. An attempt has also been made to correlate the wear rate with H/E ratio of the developed coating.

2. Experimental

TiCN coatings with compositional gradients were deposited on a X4Cr5MoWSiV hot-work tool steel substrate using a PACVD coating system equipped with a voltage-controlled pulse generator.

During coating, process parameters such as gas flow ratio, wall temperature, voltage duration of pulse-on and pulse-off time and total pressure were monitored. H_2, Ar, N_2 and CH_4 gases and $TiCl_4$ vapor were used as process gases for coating deposition. Total pressure was kept at 2 mbar and substrate temperature was controlled at 470°C to avoid exceeding the tempering temperature of the hot-work tool steel. Plasma nitriding was used as pre-treatment to decrease hardness gradient between substrate and coating [17, 18]. The processing parameters for deposition are listed in Table 1. The N_2/CH_4 gas flow ratio was defined CH_4 / (CH_4+N_2). The film morphology studied by scanning electron microscopy (SEM) and atomic force microscopy (AFM). Hardness, elastic modulus and friction coefficients of films were determined by nanoindentation test.

The nanohardness (H) and modulus of elasticity (E) have been calculated from the loading–unloading curve using Oliver and Pharr analysis. In general, the hardness, H, is defined as the ratio of the peak load, P_{max}, to the projected area of the indented impression, A_c, i.e.

$H= P_{max}/A_c$ and $A_c = f(h_c^2) = 24.5hc^2$ for Berkovich indenter, where h_c is the contact depth at peak load According to the analysis of Oliver and Pharr, h_c can be determined from the following equation:

$$h_c = h_{\max} - \varepsilon \frac{p_{\max}}{S} \quad (1)$$

Where h_{max} is the displacement measured at peak load. The second term on the right-hand side of the equation represents displacement of the specimen surface at the perimeter of contact at peak load. The term ε is a constant related to the indenter geometry while S is the unloading stiffness at maximum load. S can be calculated from loading–unloading curve as

$$S = \left(\frac{dP}{dh}\right)_{h=h_{\max}} = \gamma\left(\frac{2}{\sqrt{\pi}}\right)E_r\sqrt{A} \quad (2)$$

The term γ, a correction factor due to lack of axial symmetry. The reduced modulus E_r is defined as

$$\frac{1}{E_r} = \frac{1-\nu_i^{\,2}}{E_i} + \frac{1-\nu_s^{\,2}}{E_s} \quad (3)$$

Where, E_i, ν_i, E_r and ν_r, represent the Young's module and Poisson's ratios of the indenter, i and sample, s, respectively.

Hence, by determining the unloading stiffness (S) at the peak load from loading–unloading curve, hardness (H) and modulus of elasticity (E) can be evaluated.

Atomic force microscopy (AFM) (Carl Zeiss supra-40) has been used to evaluate dimensions, area and morphology of nanoindentation impression.

Table 1. PACVD parameters.

Parameters	Value
Pulsed voltage	650 V
Duty cycle	33%
Temperature	470°C
PACVD time	120 min
$CH_4/(CH_4+N_2)$ flow ratio	50%
Total pressure	2 mbar
TiN coating temperature	470°C
TiN coating time	120 min
nitriding time	120 min
nitriding temperature	470°C

3. Results and discussions

Fig.1 shows the microstructures of the cross-sections of the coatings produced with voltage 650 W for plasma and current 2 mA, respectively. It can be observed from these SEM images (Fig.1) that, for the sample processed the microstructure exhibits considerable amount of porosity at the cross-section of the coating.

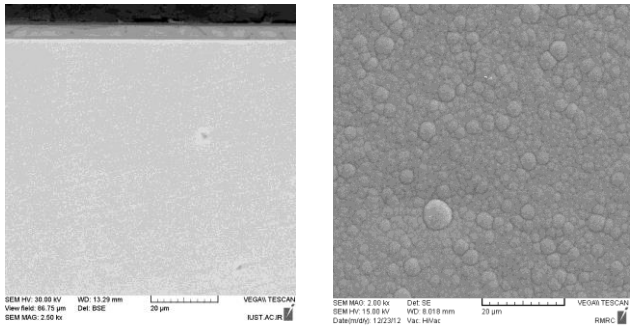

a) b)

Fig.1.SEM photo-micrographs of transverse cross-sections of the coatings deposited with plasma (a) cross section and (b) morphology.

Similar observations have been made by Zhao and Debroy [32]. Fig.1 shows the microstructures of the coatings at the transverse cross sections observed under SEM at high magnification. Thus, the deposition rate of the gas is relatively faster after the forming plasma media, which results in the formation of finer microstructure. Similar phenomena have been observed by other research groups [33–35].

Fig.2 illustrates the relation between the load and displacement during loading–unloading of the indenter with 38mN loads on the coating deposited on AISI H12 steel. Corresponding calculated values of E and H reveal that their variations with the applied loads were insignificant. Consequently, to simplify the experimental conditions, all data obtained with 38 mN load has been considered for property evaluation.

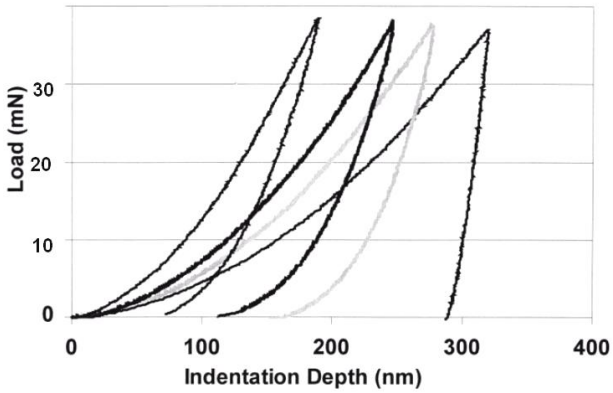

Fig.2. *Load–displacement curves during loading and unloading of the indenter with100 mN load for TiCNcoating.*

Fig.3 shows the AFM photomicrograph of the nanoindentation obtained with 38mN load on surface of the composite coating developed. As evident from the micrograph, size of indentation is large and appropriately covering various individual phases present inside the microstructure of the coating, which confirms that the elastic modulus and nano-hardness values obtained are applicable for the composite coating as a whole and not for individual phases.

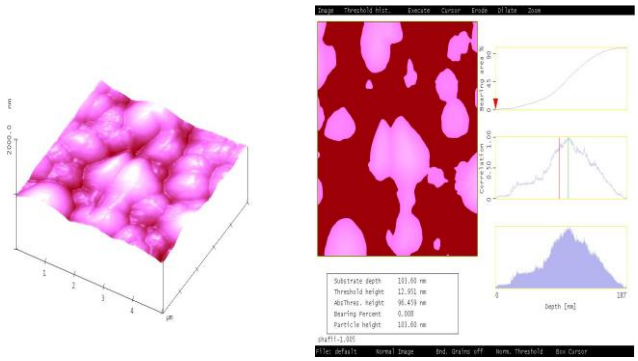

Fig.3. *AFM image of nanoindentation obtained with 100mN load on polished top surface of the coating.*

Table 2 presents the average modulus of elasticity (E) and nanohardness values obtained from the load-displacement curves (with 38mN load) for various coatings developed. E value of the coatings was found to be within the range 96.3 – 99.2 GPa. It emerges that elastic modulus values of developed coatings are considerably lower than those of individual ceramics. It is plausible that presence of some meta-stable phases in the microstructure of the coating coupled with grain refinement due to rapid depositing involved in the process may have resulted in reduction of E value of the composite coating developed. Nanohardness (H) values of the composite coating obtained are in the range of 10.6 – 13.2 GPa. These results are observed to be quite similar to that of previously reported average Vickers micro-hardness values obtained at the cross section of the TiCN coatings [38]. From these data it is clear that the developed TiCN coating is exhibiting high hardness with low modulus of elasticity. It is well known that maximizing coating hardness will be beneficial in terms of enhanced resistance to plastic deformation. It has been found that [30] lower elastic modulus will be particularly beneficial, especially if E can be adjusted to closely match that of the underlying substrate material, thus minimizing coating/substrate interfacial stress discontinuities under an applied load, allowing the coating to deflect in consideration with the substrate without cracking or debonding.
This is beneficial for the coating–substrate system as it reduces the possibility of residual stress development at the coating–substrate interface. It has been found from the literature [30] that, a lower value of the elastic modulus will be particularly beneficial for a coating, especially if E can be adjusted to closely match that of the underlying substrate material, thus minimizing coating–substrate

interfacial stress discontinuities under an applied load, allowing the coating to deflect in consonance with the substrate without cracking or debonding.
H/E ratios for various coating microstructure have been calculated and plotted against processing parameters employed. This could be possible due to greater extent of improvement in hardness of the coating due to micro structural refinement accompanied with reduction in elastic modulus values, thus indicating the possibility of tailoring the microstructure of the coating developed for enhanced mechanical properties with better coating integrity and strength.
Stiffness values of the composite coatings calculated according to the model proposed by Evans and Wilshaw [32] are found to be in the range of 67.8–70.6 MPam1/2 (as shown in Table 2). This range is observed to be higher than that of monolithic Al_2O_3, TiB_2 or TiC materials and comparable reasonably well with reported fracture toughness values of ceramic matrix composite developed by employing some conventional processes. For the present case, TiCN coating exhibits higher fracture toughness than the respective fracture toughness values of TiN,TiC[7].
Table.2 indicates that the strength of the bond between coating and interface is high. A similar study was performed by Raimondi et al. [9] for a qualitative measurement of interfacial strength of the coating surface interface for a TiCN-Fe composite coating produced with plasma surface engineering process.

Table.2: Hardness, modulus of elasticity (E) and fracture toughness values for some individual ceramics and ceramic composites.

Coating	*H (GPa)*	*E (Gpa)*	*E/H*	*Stiffness (MPam1/2)*	*Strength of bond (MPa)*
TiCN	*11.6–13.9*	*97.3–99.2*	*7-8.55*	*67.8–70.6*	*39.6*

4. Conclusion

The modulus of elasticity (E) of the developed coating has been found to be in the range of 97.3–99.2 GPa, which is lower than those of the individual monolithic ceramics. Hence, the difference between the values of E of the developed composite coating and its substrate is relatively lower than those between the ceramic coatings and their respective substrates. This leads to a distinct improvement in coating quality as a low difference in the E values of the coating and substrate is beneficial for proper coating–substrate combination. Nano-hardness (H) value of the developed composite coating is in the order of 11.6–13.9 GPa and is found to increase with the increase in laser scanning speed owing to refined microstructure. Fracture toughness of the coating is found to be in the range of 67.8–70.6 MPam1/2, which is higher than those of individual ceramics and compares well with some of the reported fracture toughness values of ceramic coatings developed by adopting conventional methods. Most notably, the wear rate of the developed composite coatings is found to have a decreasing trend with increase in H/E values.

5. Acknowledgements

Financial support of Iran University of Science and Technology is highly appreciated.

References

[1] K.T. Rie, A. Gebauer, J. Woehle, H.K. To¨nshoff, C. Blawit, Syn thesis of TiN/TiCN/TiC layer systems on steel and cermet substrates by PACVD, Surf. Coat. Technol. 375–381, **74/75**, (1995).
[2] P. Hedenqvist, M. Olsson, P. Wallen, A. Kassman, S. Hogmark, S. Jacobson, How TiN coatings improve the performance of high speed tools, Surf. Coat. Technol. 243–256, **41,** (1990).
[3] J.E. Sundgren, Structure and properties of TiN coatings, Thin Solid Films. 21–44, **128,** (1985).

[4] K.T. Rie, A. Gebauer, J. Woehle, Investigation of PA-CVD of TiN: relations between process parameters spectroscopic measurements and layer properties, Surf. Coat. Technol. 385–388 **, 60,** (1993).
[5] Y. Ishii, H. Ohtsu, T. Adachi, H. Ichimura, K. Kobayashi, TiN film formation by plasma chemical vapour deposition and its plasma diagnostics, Surf. Coat. Technol. 279–283, **49**, (1991).
[6] I. Dion, F. Rouais, L. Trut, C. Baquey, J.R. Monties, P. Havlik, Biomaterials. 169, **14**, (1993).
[7] I. Dion, X. Roques, N. More, L. Labrousse, J. Caix, F. Lefebvre, F. Rouais, J. Gautreau, C.Baquey, Biomaterials. 712, **14,** (1993).
[8] J. Narayan, W.D. Fan, R.J. Narayan, P. Tiwari, H.H. Stadelmaier, Mat. Sci. Eng. B 5, **25**, (1994).
[9] M.T. Raimondi, R. Pietrabissa, Biomaterials. 907, **21,** (2000).
[10] F. Mestral, F. Thevenot, J. Mater. Sci. 5547–5560, **26**, (1991).
[11] J. Senthil Selvan, K. Subramanian, A.K. Nath, H. Kumar, C. Ramachandra, S.P.Ravindranathan, Mater. Sci. Eng. A 178–187, **260,** (1999).
[12] Y.S. Tian, C.Z. Chen, L.B. Chen, J.H. Liu, T.Q. Lei, J. Mater. Sci. 4387–4390, **40**, (2005).
[13] W. Xibao, L. Yong, Y. Songlan, Surf. Coat. Technol. 209–216, **137**, (2001).
[14] H.C. Man, S. Zhang, F.T. Cheng, X. Guo, Surf. Coat. Technol. 4961–4966, **200,** (2006).
[15] S. Liu, W. Zhang, J. Alloys Compd. 146–150, **391**, (2005).
[16] H. Park, K. Nakata, S. Tomida, J. Mater. Sci. 747–755, **35,** (2000).
[17] A. Singh, N.B. Dahotre, J. Mater. Sci. 4553–4560, **39**, (2004).
[18] B. Bhushan, in: Bharat Bhushan (Ed.), Nanomechanical Properties of Solid Surfaces and Thin Films, Handbook of Micro/Nanotribology, CRC Press LLC, Boca Raton, 1999.
[19] W.C. Oliver, G.M. Pharr, J. Mater. Res. 1564–1580, **7,** (1992).
[20] H.C. Barshilia, N. Selvakumar, K.S. Rajam, D.V. Sridhara Rao, K. Muraleedharan, Thin Solid Films. 6071–6078, **516,** (2008).
[21] A.C. Fischer-Cripps, P. Karvaˇınkovaˇı, S. Veprˇek, Surf. Coat. Technol. 5645–5654, **200,** (2006).
[22] K.S.S.E. Raju, S. Bysakh, M.A. Sumesh, S.V. Kamat, S. Mohan, Mater. Sci. Eng. A. **476,** 267–273 (2008).
[23] J. Sjolen, L. Karlsson, S. Braun, R. Murdey, A. Horling, L. Hultman, Surf. Coat.Technol. 6392–6403, **201,** (2007).
[24] J. Gong, H. Miao, Z. Peng, L. Qi, Mater. Sci. Eng. A 140–145, **354**, (2003).
[25] H. Ichimura, I. Ando, Surf. Coat. Technol. 88–93, **145,** (2001).
[26] J. Musil, F. Kunc, H. Zeman, H. Polaˇıkova, Surf. Coat. Technol. 304–313, **154**, (2002).
[27] A. Biswas, L. Li, U.K. Chatterjee, I. Manna, S.K. Pabi, J. Dutta Majumdar, Scr. Mater. 239–242, **59** , (2008).
[28] A. Agarwal, N.B. Dahotre, Metall. Mater. Trans. A 401–408, **31**, (2000).
[29] J. Xu, W. Liu, Wear 486–492, **260,** (2006).
[30] A. Leyland, A. Matthews, Wear 1–11, **246,** (2000).
[31] A.G. Evans, T.R. Wilshaw, Acta Metall. 939–956, **24,** (1976).
[32] H. Zhao, T. Debroy, Welding Res. Suppl. 204–210(2001).
[33] P. Kadolkar, N.B. Dahoter, Appl. Surf. Sci. 222–233, **199,** (2002).
[34] M.H. McCay, N.B. Dahotre, J.A. Hopkins, T.D. Mccay, M.A. Riley, J. Mater. Sci. 5789–5802, **34,** (1999).
[35] Y.S. Tian, C.Z. Chen, L.B. Chen, L.X. Chen, Appl. Surf. Sci. 1494–1499, **253**, (2006).